

## Mode coupling theory and fragile to strong transition in supercooled TIP4P/2005 water

M. De Marzio, G. Camisasca, M. Rovere, and P. Gallo

Citation: *The Journal of Chemical Physics* **144**, 074503 (2016); doi: 10.1063/1.4941946

View online: <http://dx.doi.org/10.1063/1.4941946>

View Table of Contents: <http://scitation.aip.org/content/aip/journal/jcp/144/7?ver=pdfcov>

Published by the **AIP Publishing**

---

### Articles you may be interested in

[Fragile to strong crossover at the Widom line in supercooled aqueous solutions of NaCl](#)

*J. Chem. Phys.* **139**, 204503 (2013); 10.1063/1.4832382

[A molecular dynamics study of the equation of state and the structure of supercooled aqueous solutions of methanol](#)

*J. Chem. Phys.* **137**, 184503 (2012); 10.1063/1.4767060

[Mode coupling and fragile to strong transition in supercooled TIP4P water](#)

*J. Chem. Phys.* **137**, 164503 (2012); 10.1063/1.4759262

[Widom line and the liquid–liquid critical point for the TIP4P/2005 water model](#)

*J. Chem. Phys.* **133**, 234502 (2010); 10.1063/1.3506860

[Fragile-to-strong liquid transition in deeply supercooled confined water](#)

*J. Chem. Phys.* **121**, 10843 (2004); 10.1063/1.1832595

---



**AIP Applied Physics Reviews**

# NEW Special Topic Sections

**NOW ONLINE**  
Lithium Niobate Properties and Applications:  
Reviews of Emerging Trends

**AIP** | Applied Physics Reviews

# Mode coupling theory and fragile to strong transition in supercooled TIP4P/2005 water

M. De Marzio,<sup>1</sup> G. Camisasca,<sup>1</sup> M. Rovere,<sup>1</sup> and P. Gallo<sup>2,a)</sup>

<sup>1</sup>Dipartimento di Matematica e Fisica, Università “Roma Tre,” Via della Vasca Navale 84, 00146 Roma, Italy

<sup>2</sup>Dipartimento di Matematica e Fisica, Università “Roma Tre” and INFN Sezione Roma Tre, Via della Vasca Navale 84, 00146 Roma, Italy

(Received 7 October 2015; accepted 1 February 2016; published online 19 February 2016)

We study by molecular dynamics simulations supercooled water with the TIP4P/2005 potential. This model is able to predict many properties of water in a large range of the thermodynamic space in agreement with experiments. We explore the dynamical behavior and, in particular, the self intermediate scattering function of the oxygen atoms. We find that the structural relaxation in the range of mild supercooling is in agreement with the Mode Coupling Theory (MCT). The ideal MCT crossover takes place at decreasing temperature with increasing density. Deviations from the MCT behavior are found upon further supercooling. A crossover from the MCT, fragile, regime to a strong, Arrhenius, regime is found and it is connected to the presence of a liquid-liquid phase transition and the Widom line emanating from the liquid-liquid critical point. © 2016 AIP Publishing LLC. [<http://dx.doi.org/10.1063/1.4941946>]

## I. INTRODUCTION

Water is one of the most abundant compound in the world and at the same time a most anomalous substance. A huge amount of theoretical and experimental research has been developed to understand the properties of liquid water that distinguish it from other liquids. One of its anomalies is the presence of a temperature of maximum density (TMD), a locus of thermodynamic space where the density reaches a maximum. Besides the TMD, another interesting peculiarity is the appearance in the supercooled regime of an increase of thermodynamic response functions, which seem to diverge with a power law, typical of phase transitions.<sup>1</sup> From an experimental point of view, this thermodynamic region is in principle not forbidden<sup>2</sup> but in deep supercooled region is difficult to explore, because metastable liquid water tends to nucleate, and this is why it is called “no-man’s land.”<sup>3</sup> For this reason, a lot of theoretical and computational efforts have been done to investigate and understand the origin of these divergences.

Various scenarios have been hypothesized for explaining water’s anomalies. Among the different theoretical models the singularity free scenario<sup>4,5</sup> interprets the increase of the thermodynamic response functions as a necessary consequence of the TMD anomaly. Calculations done with lattice models able to reproduce this scenario show a thermodynamically consistent interpretation of the phase behavior of metastable water so it cannot be excluded as a possible explanation of the anomalies of the response functions of supercooled water.

The interpretation that has received by far the greatest attention is the liquid-liquid critical point (LLCP) scenario.

This scenario was proposed based on the existence of the LLCP in ST2 water by Poole, Sciortino, Essmann and Stanley.<sup>6</sup>

The LLCP hypothesis matches with glassy water polyamorphism. Experiments have evidenced the existence of two phases of glassy water, the high density amorphous ice (HDA) and the low density amorphous ice (LDA).<sup>7–10</sup> HDA and LDA would evolve at high temperature in a high density liquid (HDL) and a low density liquid (LDL), respectively,<sup>10</sup> and their coexistence curve would terminate in the LLCP, approximately located at  $T \sim 220$  K and  $P \sim 100$  MPa.<sup>11,12</sup>

Computational studies have shown that for many popular water models the LLCP is present.<sup>6,13–18</sup>

The liquid-liquid phase transition has been also confirmed by recent more extensive computations based on free energy calculations.<sup>19–30</sup> Theoretical scaling analysis of the LLCP gives also a consistent scenario.<sup>1,31,32</sup>

Generally speaking, in presence of a critical point, upon approaching it from the one phase region the response functions exhibit loci of maxima. As it is the case in critical phenomena,<sup>33</sup> it is expected within the LLCP scenario that those maxima collapse on the Widom line,<sup>34,35</sup> defined as the locus of maximum correlation length upon moving toward the critical point from the one phase region. The maxima of those response functions collapse on the same line on approaching the critical point because they become proportional to power laws of the correlation length. How close to the critical point they collapse depends on the system.<sup>36–39</sup> Since it is difficult to locate the Widom line from the behavior of the correlation length<sup>38</sup> its location from response function maxima is often used as a plausible approximation in supercooled water. In particular, the Widom line has been individuated from the maxima of the specific heat or of the isothermal compressibility in a number of computer simulations.<sup>17,18,34</sup>

<sup>a)</sup>gallop@fis.uniroma3.it

We note that experiments and computer simulations on several popular water all atoms potentials in supercritical water show that the maxima of the response functions collapse on the Widom line well above the liquid gas critical point.<sup>40,41</sup> In TIP4P/2005, in particular, they collapse for a range of circa 30 K in temperature above the liquid gas critical point.<sup>40</sup>

By considering the LLCPP to be the source of its thermodynamic peculiarities a consistent description of the phenomenology of supercooled water is obtained.

Less attention has been devoted to the dynamical aspects of this metastable region and to a connection between dynamics and thermodynamic singularities. Already in 1996 it was shown that SPC/E supercooled water behaves like simple glass formers,<sup>42,43</sup> following the Mode Coupling Theory (MCT) of glassy dynamics.<sup>44</sup> In particular, it was shown that the singular temperature, which is the temperature of the apparent divergence of the thermodynamic quantities like specific heat upon supercooling, coincides with the MCT temperature  $T_C$  showing a connection between dynamics and thermodynamics. Time resolved spectroscopy experiments have later confirmed that water behaves *à la* Mode Coupling and that  $T_C$  coincides with the singular temperature.<sup>45</sup> MCT for supercooled water has been also tested for other water models like TIP4P, both in bulk water<sup>46</sup> and in aqueous solutions,<sup>47</sup> and in SPC/E confined water.<sup>48–51</sup> The MCT power law behavior has been found also in very recent experiments measuring with dynamic differential microscopy diffusion coefficients and viscosities.<sup>52</sup>

MCT can be tested studying the density correlators.<sup>42,43</sup> Their shape allows one to find the MCT temperature  $T_C$  and scaling relationships among the exponents involved in the theory. The region in which the supercooled liquid follows MCT is associated to the fragile behavior.  $T_C$  is the temperature below which structural relaxations are frozen in the liquid and diffusion can occur only via hopping, e.g., activated, processes.<sup>44</sup> Most glass formers show a crossover from the fragile behavior to the hopping regime which is called strong regime.

Early computer simulations of water using SPC/E potential found a fragile to strong crossover (FSC).<sup>53</sup> The FSC behavior was confirmed by experiments in confined water<sup>54,55</sup> that additionally found that this crossover as a function of pressure is pointing to the region where the LLCPP has been predicted to be located.<sup>11,12</sup> The FSC has been found to happen at the crossing of the Widom line for ST2, TIP5P, and a primitive model, the Jagla model.<sup>34</sup> Experiments in confinement have also shown a peak of the specific heat in correspondence of the FSC.<sup>56</sup> Besides it was shown by computer simulations that water in hydrophilic confinement has a bulk-like behavior and that upon supercooling the FSC occurs in correspondence with a peak of the specific heat which can be considered to a good approximation as a proxy for the Widom line.<sup>50,51,57</sup> The FSC has been found to occur upon crossing the Widom line also for TIP4P bulk water,<sup>46</sup> for TIP4P aqueous solutions of electrolytes,<sup>47</sup> and for solvophobic solutions.<sup>58</sup>

All these aspects of thermodynamics and dynamics of supercooled water represent an incentive to investigate if the MCT behavior and the coincidence between FSC and Widom

Line are present in TIP4P/2005<sup>59</sup> which is currently one of the most popular water model potentials. TIP4P/2005 reproduces with very high quality the TMD curve<sup>60</sup> and low temperatures properties of stable water, like ice polymorphism,<sup>59</sup> much better than TIP5P and SPC/E. It also shows the anomalous increase of thermodynamic response functions<sup>60</sup> and the existence of a Widom Line that terminates at the LLCPP.<sup>18</sup> It is also interesting that TIP4P/2005 and TIP4P show a slope of the diffusion coefficients as function of temperature in good agreement with experiments. TIP4P/2005 values of the diffusion coefficients are close to the experimental values, while TIP4P predicts faster diffusion coefficients.<sup>61</sup>

In this paper, we study the structural relaxation of TIP4P/2005 water upon supercooling to test the MCT behavior, to find its range of validity and to discover the occurrence of a crossover to a strong behavior at the crossing of the  $c_V$  maxima line, taken, as we will show, as a good approximation of the Widom line. In Sec. II, we describe the model and the simulation details. In Sec. III, we analyze the intermediate scattering function in terms of MCT. In Sec. IV, we study the MCT transition and the FSC. In Sec. V, we show the connection between the FSC and the Widom line and we make a comparison with the TIP4P model. Sec. VI is devoted to the conclusions.

## II. MODEL AND SIMULATION METHODS

We perform molecular dynamics simulations of water molecules interacting with the TIP4P/2005 potential. The molecule is represented as two positive charged hydrogens with  $q_H = 0.5564e$  and a neutral oxygen which interacts only through a single Lennard-Jones (LJ) force with  $\sigma = 3.159 \text{ \AA}$  and  $\epsilon/k_B = 93.2 \text{ K}$ . A negative charged site  $M$  with  $q_M = -2q_H$  is placed along the bisector of the  $H-O-H$  angle and coplanar with the oxygen and hydrogens at distance  $0.1546 \text{ \AA}$  from the oxygen. This four-site potential has the same geometry of TIP4P potential but it has different site charges and LJ parameters.

We simulated a cubic box of 512 molecules at four different densities,  $\rho = 0.95 \text{ g/cm}^3$ ,  $\rho = 0.98 \text{ g/cm}^3$ ,  $\rho = 1.00 \text{ g/cm}^3$ , and  $\rho = 1.03 \text{ g/cm}^3$ . Correspondingly the box lengths go from  $25.26 \text{ \AA}$  to  $24.59 \text{ \AA}$ . The temperatures investigated span from 300 K to 195 K.

All the simulations are made with molecular dynamics parallel Gromacs package 4.5.5.<sup>62</sup> A time step of 1 fs was used. The LJ potential has a cutoff distance of  $9.5 \text{ \AA}$ . The Coulomb interactions have been implemented with the Ewald method. In particular, the potential is truncated at  $9.5 \text{ \AA}$  and the Particle Mesh Ewald (PME) algorithm was used with a Fourier spacing of  $1 \text{ \AA}$  and a fourth degree polynomial. The system has been equilibrated with Berendsen thermostat. During the production runs, the heat bath of Berendsen with a longer relaxation time is used to prevent any energy drift that would be unavoidable in the NVE ensemble for such long runs (see also Ref. 53).

A total of 39 state points was investigated. For the lowest temperature investigated, the longest run executed is a production run of 200 ns. The total computer time of our study on a single core would have been of 2.5 yr.

### III. INTERMEDIATE SCATTERING FUNCTIONS AND MODE COUPLING THEORY

In order to test MCT for TIP4P/2005 water, we calculated for the four densities in the range of temperatures mentioned above the oxygen self intermediate scattering functions (SISF), which are the Fourier transforms of the van Hove self correlation function

$$F_s(Q, t) = \frac{1}{N} \left\langle \sum_i e^{i\vec{Q} \cdot [\vec{R}_{O_i}(t) - \vec{R}_{O_i}(0)]} \right\rangle. \quad (1)$$

The calculations were done at the first peak of the oxygen-oxygen static structure factor  $Q_0 = 2.25 \text{ \AA}^{-1}$ , where the MCT features of this correlator are best evident. The results are reported in Fig. 1.

As predicted by mode coupling theory, a two step relaxation scenario is observed in the SISF as supercooling proceeds. The early time region, which characterizes

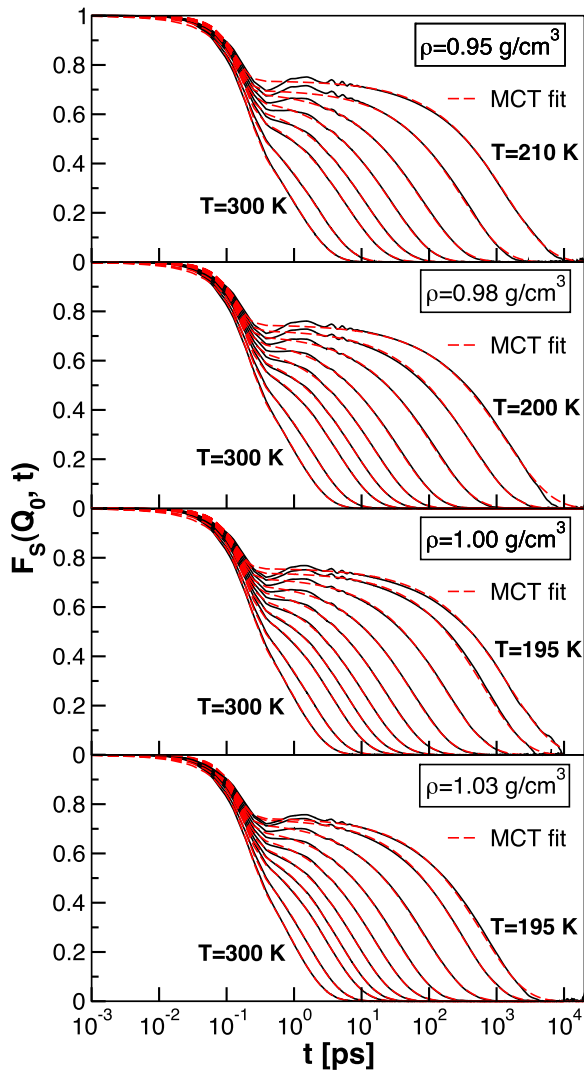


FIG. 1. Oxygen self intermediate scattering functions for different temperatures calculated at the maximum of the static structure factor for the four different densities indicated. The temperatures investigated for  $\rho = 0.95 \text{ g/cm}^3$  are  $T = 300, 280, 260, 250, 240, 230, 220, 210 \text{ K}$ . For  $\rho = 0.98 \text{ g/cm}^3$  we added  $T = 200 \text{ K}$  and for  $\rho = 1.00 \text{ g/cm}^3$  and  $\rho = 1.03 \text{ g/cm}^3$  we further added  $T = 195 \text{ K}$ . The black solid lines are the MD results and the dashed red lines are the fits to Eq. (2).

microscopic time scale, is the initial ballistic decay of the single particle dynamics. At decreasing temperature, an intermediate regime, called  $\beta$  relaxation regime, develops and evolves from a simple inflection point to a constant plateau for the lower temperatures. In this time interval, the particle is trapped in a “cage” formed by the nearest neighbors and is locked in a confined spatial region. When the cages relax the SISF enters in the so-called  $\alpha$  relaxation region described in its late part by a stretched exponential decay.

When a liquid follows MCT predictions it was shown that the overall curves can be fitted with the formula<sup>42,43</sup>

$$f(Q, t) = (1 - A(Q)) \exp[-(t/\tau_s)^2] + A(Q) \exp[-(t/\tau)^\beta], \quad (2)$$

where  $\tau_s$  is the characteristic time related to the short time fast relaxation and  $\tau$  and  $\beta$  are, respectively, the  $\alpha$  relaxation time and the Kohlrausch exponent of the long time stretched exponential decay of the SISF. The coefficient  $A(Q)$  is the Lamb-Mossbauer factor.<sup>44</sup> It corresponds to the height of the plateau and it is related to the cage dimension.

The values of the parameters of the fit are reported in Table I for the density  $\rho = 1.00 \text{ g/cm}^3$ . In agreement with MCT predictions, the parameters of the  $\alpha$  relaxation show a strong temperature dependence. In fact, for each density the SISF decays more slowly upon decreasing temperature as it is clear also from the trend of  $\tau$  and  $\beta$ . This behavior reflects the fact that the dynamics is progressively slowing down and the system’s capability to rearrange itself is reducing. Moreover, upon cooling the system, the particle stays in the cage for longer times, as it can be seen from the increasing length of the plateau.

We now describe a feature that is one of the manifestation of water peculiar behavior, the diffusion anomaly.<sup>53,60,63–66</sup> The diffusion anomaly is usually present for densities from 0.9 to 1.15  $\text{g/cm}^3$ . For supercooled temperatures upon decreasing density along isotherms, at variance with to what expected for simple liquids, the diffusion coefficient decreases<sup>65</sup> and correspondingly  $\tau$  increases.

In Fig. 2, we plot the SISF for the four densities investigated for  $T = 210 \text{ K}$ . Upon comparing different densities at the same temperature, it is evident that at lower densities the motion of the particle is slower.

In Fig. 3, we show this diffusion anomaly in the range of densities investigated for the TIP4P/2005 by plotting the  $\alpha$  relaxation time as a function of density for the state points

TABLE I. Fitting parameters of the SISF with Eq. (2) for the density  $\rho = 1.00 \text{ g/cm}^3$ .

$T$ (K)	$A$	$\tau_s$ (ps)	$\tau$ (ps)	$\beta$
300	0.6836	0.2073	0.9216	0.8395
280	0.6636	0.1947	1.615	0.8044
260	0.6464	0.1836	3.607	0.8014
250	0.6523	0.1778	6.072	0.7853
240	0.6716	0.1699	10.95	0.7567
230	0.6889	0.1618	22.55	0.7356
220	0.7000	0.1585	55.31	0.7252
210	0.7216	0.1514	173.7	0.7065
200	0.7400	0.1473	658	0.7200
195	0.7580	0.1410	1547	0.6652

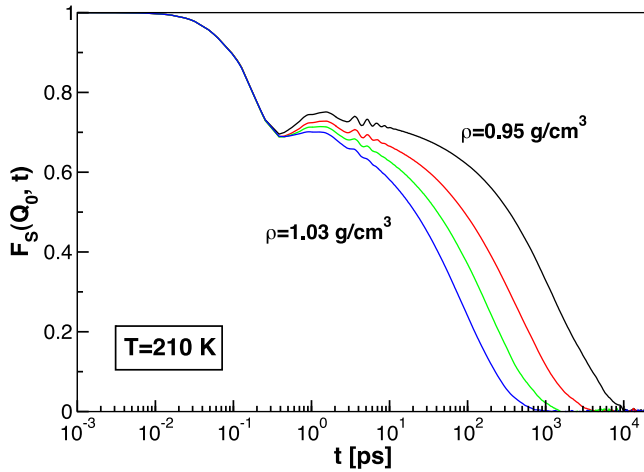


FIG. 2. Oxygen self intermediate scattering functions calculated at the maximum of the static structure factor for the four different densities investigated at the same temperature  $T = 210$  K.

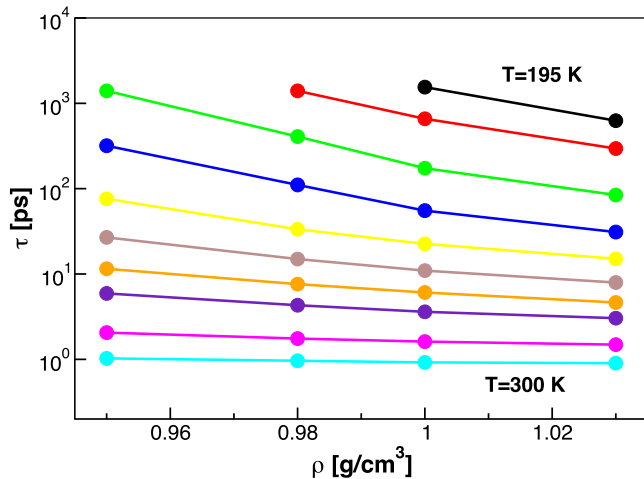


FIG. 3. Isothermal curves of  $\alpha$  relaxation time as a function of densities investigated from  $T = 300$  K to  $T = 195$  K.

ranging from  $T = 300$  K to  $T = 195$  K. Lower densities correspond to a liquid that is more close to the LDL phase and at the same time is more structural arrested. Moreover the increase of  $\tau$  with decreasing density becomes more and more pronounced upon decreasing temperature (the  $\alpha$  relaxation times are plotted on logarithmic scale). This means that at lower temperatures the progressive passage from structures with greater mobility and faster dynamics to more “frozen” structures is quicker upon decreasing density. We also observe that with respect to the TIP4P potential<sup>46</sup> the values of the  $\alpha$  relaxation time at the same temperature and density are greater, indicating that the TIP4P/2005 system has less mobility. We will discuss this point later.

The Kohlrausch exponent values are in the same range of TIP4P and decrease slowly.

#### IV. MCT TRANSITION AND FRAGILE TO STRONG CROSSOVER

MCT explains various aspects of the phenomenology of supercooled liquids. In particular, the dependence of  $\tau$  on

temperature should follow a power law:

$$\tau \sim (T - T_C)^{-\gamma}, \quad (3)$$

where  $T_C$  is the Mode Coupling temperature and  $\gamma$  is an universal exponent which should be independent from the system studied. The Eq. (3) shows that at  $T_C$ , the relaxation time  $\tau$  diverges asymptotically. This is because the temperature  $T_C$  should mark the transition from the ergodic phase of the system where the particles are able to relax definitely after the cage transient regime and the non-ergodic phase where the SISF does not decay to zero and the particle remains trapped in the frozen cage. Ideally, in this phase, the dynamics is structurally arrested and the system has vitrified. In real systems, SISF decays to zero also under  $T_C$ . This is because around this temperature, other phenomena occur in addition to the “cage effect.” In fact, even if the cage has not relaxed, the particle has the possibility to escape from it by activated processes referred as *hopping processes*.<sup>67,68</sup> When the system approaches  $T_C$  the hopping processes become more and more important and dominate the dynamics below  $T_C$ . This means that the range of validity of Eq. (3) is limited and close to the ideal glass transition hopping phenomena deviate the behavior of  $\tau$  towards a temperature dependence where  $\tau$  grows exponentially with temperature, following an Arrhenius law:

$$\tau = \tau_0 e^{E_A/k_B T}, \quad (4)$$

where  $E_A$  is the activation energy for the hopping.

In Fig. 4, we show the high temperatures MCT fit and low temperatures Arrhenius fit for each of the four densities investigated. The values of the fit parameters are shown in Table II. We note that the temperature of crossover from fragile to strong,  $T_L$ , happens at higher temperatures with respect to the MCT temperature of ideal structural arrest  $T_C$ . This is because the hopping processes start to occur when cages are still not completely frozen.

Except  $\rho = 1.03$  g/cm<sup>3</sup>, all the densities have the crossover from MCT to Arrhenius behavior. The values of fragile to strong crossover temperatures are reported in

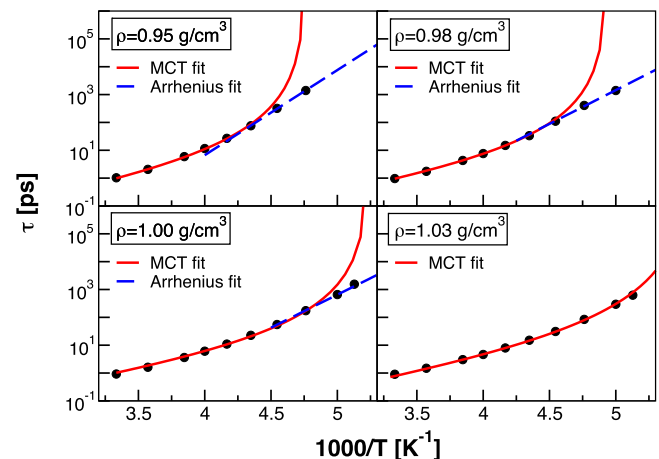


FIG. 4. Complete behavior of the  $\alpha$  relaxation time  $\tau$  versus the inverse of the temperature for the four different densities investigated. The red lines are the fit with mode coupling power law, see Eq. (3). The blue lines are the fit with the Arrhenius function, see Eq. (4).

TABLE II. Fitting parameters of MCT Eq. (3) and Arrhenius Eq. (4) for each density and correspondent fragile to strong crossover temperatures.

$\rho$ (g/cm <sup>3</sup> )	$T_C$ (K)	$\gamma$	$E_A$ (kJ/mol)	$T_L$ (K)
0.95	209.898	2.982	58.454	230
0.98	202.628	2.858	46.349	220
1.00	190.829	2.939	45.291	210
1.03	179.687	3.354	...	...

Table II. As said above, this FSC represents a transition from the state where water diffusion properties have a fragile behavior to a region where water behaves as a strong liquid. The fits of MCT are done excluding high temperatures values at which water does not yet follow the supercooled liquid dynamics. In agreement with the existence of a diffusion anomaly, we see that lower densities correspond to a more arrested liquid and correspondingly the temperatures of the ideal glass transition of MCT,  $T_C$ , increase upon decreasing density. This trend is found also for the temperatures  $T_L$ , at which the crossover occurs. For a better panoramic of the deviations from MCT, we plot in Fig. 5 in the log-log plane the inverse of  $\alpha$  relaxation time as a function of  $T - T_C$ . TIP4P/2005 diffusion coefficients  $D$  were also shown to behave consistently with MCT power law.<sup>69</sup>

A further test of the predictions of MCT and of its range of validity is provided by the time-temperature superposition principle (TTSP). Accordingly to MCT, the final part of the  $\beta$  relaxation, where the SISF is going out from the plateau and enters in the  $\alpha$  relaxation, is described by the von Schweidler law (VSL)

$$\phi_Q(t/\tau) = f_Q - h_Q \cdot (t/\tau)^b. \quad (5)$$

The parameter  $f_Q$  is the ergodicity factor,  $h_Q$  is the amplitude and the exponent  $b$  is the von Schweidler exponent. Equation (5) implies that the SISF collapses on a master curve independent from temperature if plotted against the rescaled time  $t/\tau$ . In Fig. 6 we show for each density investigated the SISFs as a function of the correspondent  $t/\tau$  and the fit

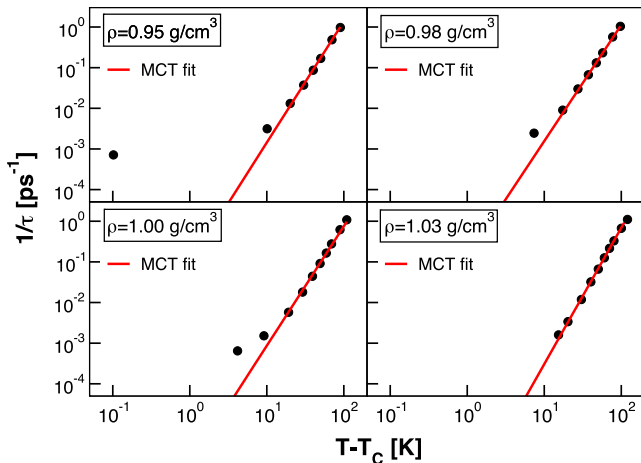


FIG. 5. Log-log plot of the inverse of the  $\alpha$  relaxation time  $1/\tau$  versus  $T - T_C$  for the four different densities investigated. The red line is the MCT fit, see Eq. (3). For each panel only the temperatures  $T > T_C$  can be shown.

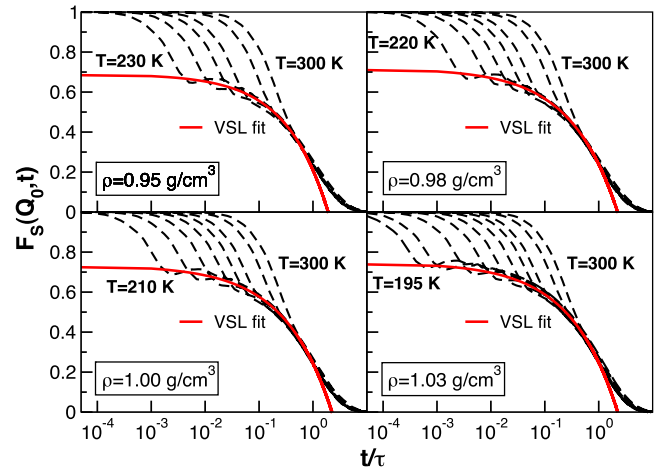


FIG. 6. SISF vs scaled time  $t/\tau$  for the four different densities in the range of temperatures where MCT holds. The red lines are the von Schweidler law fits, see Eq. (5).

with the VSL equation. It is clear that the TTSP holds for all the densities in the range of validity of MCT. The values found for  $\rho = 1$  g/cm<sup>3</sup> are  $f_Q = 0.734$ ,  $h_Q = 0.490707$  and  $b = 0.4949$  similar to the values found for other potentials.<sup>43,46</sup> The exponent  $b$  is related to the other parameter which characterizes the early part of the  $\beta$  relaxation, the critical exponent  $a$ , and to the exponent parameter  $\lambda$ , with the following relation:

$$\lambda = \frac{\Gamma^2(1+b)}{\Gamma(1+2b)} = \frac{\Gamma^2(1-a)}{\Gamma(1-2a)}, \quad (6)$$

$a$  and  $b$  parameters are also related to the power law exponent of the MCT law with a scaling equation

$$\gamma = \frac{1}{2a} + \frac{1}{2b}. \quad (7)$$

To further test the validity of MCT we calculated the exponent  $a$  from Eq. (7) and then the exponent  $\lambda$  both from  $a$  and from the  $b$  calculated independently with the VSL law. For density  $\rho = 1$  g/cm<sup>3</sup>, we obtain  $\lambda = 0.83$  from  $a$  and  $\lambda = 0.79$  from  $b$ . These values are in fairly good agreement, the slight difference can be caused by the presence of hopping phenomena, which are known to begin to occur also in the range of validity of MCT.

## V. FRAGILE TO STRONG CROSSOVER AND WIDOM LINE

As seen in Sec. IV, the dynamics of TIP4P/2005 water shows upon cooling along an isochore a crossover from a fragile, ideal, MCT behavior in the mild supercooled region to an Arrhenius behavior upon further supercooling below the temperatures  $T_L$  reported in Table II. In the Introduction, we have discussed how the phenomenon of this crossover has been connected in the literature to the presence of a liquid-liquid phase transition between two coexisting phases of a fragile high density liquid and a strong low density liquid.<sup>34,46,47,50,51,56-58</sup> Approaching the critical point from the single phase region the crossover would take place upon crossing the Widom line emanating from the LLCP. This

correspondence can be interpreted considering the FSC as a transition from a region where the system is more free to relax and rearrange itself, which is, as also seen above, a high density region and a phase where water has a slower dynamics and so has an equilibrium structure less dense. Since in water the coexistence line has a negative slope, the high temperature phase corresponds to the HDL, and the low temperature phase to the LDL.

Even though, as said above, the locus of maxima of the specific heat does not, generally speaking, necessarily coincide with the Widom Line, it is possible for TIP4P/2005 to locate the Widom line with the line of collapse of maxima of thermodynamic quantities such as the specific heat and the isothermal compressibility that diverge in approaching asymptotically the LLCP. In fact, as reported in Ref. 18, TIP4P/2005 displays a LLCP at  $T = 193$  K,  $P = 135$  MPa,  $\rho = 1.012$  g/cm<sup>3</sup> and a locus of maxima of isothermal compressibility, which roughly coincides also with the minima of expansivity and hence can be considered as a good indication of the Widom Line. As a further confirmation, also the specific heat maxima that we calculated roughly coincide with the Widom line in a range of circa 30 K.

In this work, we have calculated the specific heat at constant volume  $c_V = (\partial U/\partial T)_V$  for the four isochores investigated to trace the Widom line. Fig. 7 shows the results of MD simulations. All the densities except  $\rho = 1.03$  g/cm<sup>3</sup> have a maximum. We note that the values of the maxima of  $c_V$  decrease on approaching the region of larger fluctuations and the critical point. This behavior is due to cancellation effects, as already discussed for TIP5P water in Ref. 70. for  $c_P$ . Also  $c_V$  shows this behavior, in fact  $c_V = (\partial U/\partial T)_P - (\partial U/\partial V)_T(\partial V/\partial T)_P$ .  $(\partial V/\partial T)_P < 0$  in the density anomaly region and diverges at the critical point.  $(\partial U/\partial V)_T < 0$  as calculated from our data, see also Ref. 71. Therefore both first and second term of  $c_V$  diverge at the critical point with opposite signs.

In Fig. 8, we plot the LLCP, the  $c_V$  maxima, the FSC and the TMD curve of TIP4P/2005 in the plane  $\rho$ - $T$ . It is clear that,

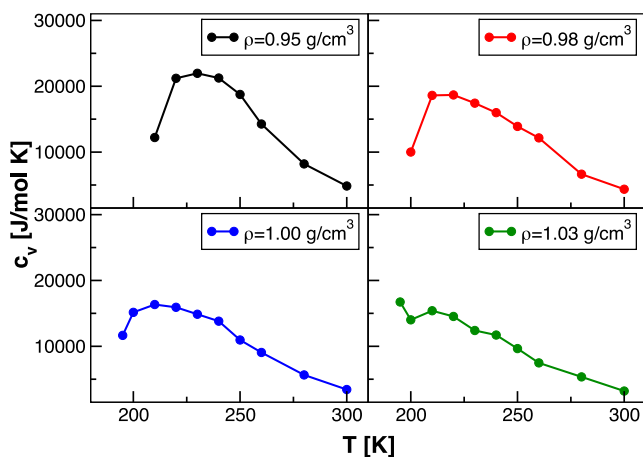


FIG. 7. Plot of the isochoric specific heat,  $c_V$ , for the four different densities investigated as a function of temperature. For each density under the critical density,  $\rho_C = 1.012$  g/cm<sup>3</sup>, a maximum appears. For the density  $\rho = 1.03$  g/cm<sup>3</sup>, above the critical density,  $c_V$  continues to increase upon lowering temperature down to the lowest temperature investigated.

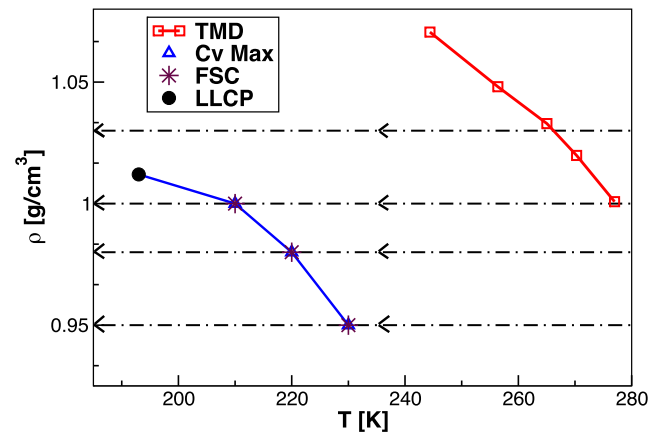


FIG. 8. Results in the  $\rho$ - $T$  plane. The horizontal dashed lines indicate the different isochores calculated with MD simulations.  $c_V$  maxima are empty triangles, fragile to strong crossovers are stars, the LLCP is the full circle and the TMD are squares, the continuous lines are guides for the eye.

within statistical fluctuations, the points of the FSC coincide with the  $c_V$  maxima taken as a proxy for the Widom line. The relation between the FSC and the Widom line shows an important connection between thermodynamic and dynamical properties of the system.

At the density  $\rho = 1.03$  g/cm<sup>3</sup> the system lies above the LLCP inside the HDL region and does not cross the Widom line. We see that it does not exhibit a  $c_V$  maximum and a FSC crossover down to the lowest temperature investigated. The anomalous increase of specific heat might be due to the approach to the glass transition temperature as the system is only 15 K away from the glass transition temperature estimated by Abascal and Vega.<sup>18</sup> We also note that due to the approach to the glass transition temperature hopping processes could become active at lower temperatures also for this isochore.

In Fig. 9, we report the significant thermodynamic curves together with the FSC for the potentials TIP4P and

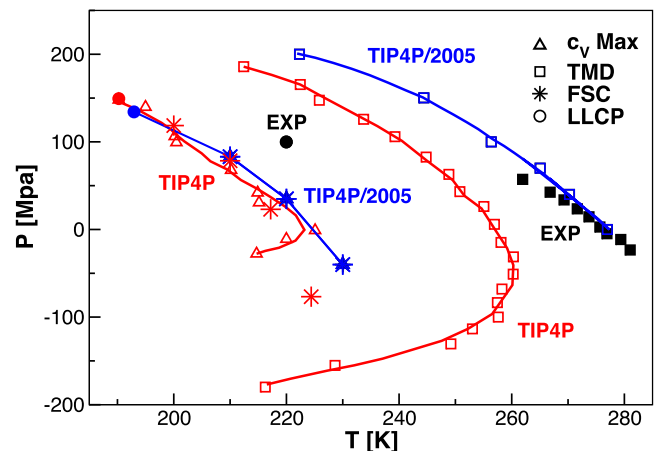


FIG. 9. Plot in the  $P$ - $T$  plane of the maximum of response functions  $c_V$  (triangle up) together with the FSC (stars) and TMD lines (squares) for TIP4P (red symbols and lines)<sup>17,46</sup> and TIP4P/2005 (blue symbols and lines) potentials. TIP4P/2005 TMD is from Ref. 18. Black squares are experimental results for the TMD line. LLCP are filled circle symbols. The experimental LLCP refers to the estimated value in Refs. 11 and 12.

TIP4P/2005 in the plane P-T. The experimental curve of the TMD is also reported in the available range.

The TIP4P/2005 shows a TMD line in agreement with experiments, while the TMD of TIP4P water is rigidly shifted toward lower temperatures and pressures. Both TIP4P and TIP4P/2005 predict a similar range of existence for the stable liquid phase. In the supercooled phase both the models predict similar location for the LLC. The dynamics of TIP4P/2005 however results to be slower at equal temperature with respect to the TIP4P dynamics in agreement with previous calculations of the diffusion coefficient as function of temperature.<sup>46,61</sup> In spite of this difference, the Widom lines and the FSC curves of the two models are very close at positive pressure in approaching the respective LLC.

It has been found that the TIP4P/2005 and TIP4P have similar crystalline phase diagrams and their performance are much better with respect to other potentials. TIP4P/2005 is more in agreement with experiments. The reason is attributed to the difference in the charge distribution for which TIP4P/2005 gives a better description of the orientational order.<sup>61</sup> As the system approaches the deep supercooled region phase it is possible that this difference becomes less relevant and the two models give similar prediction for quantities averaged on long time. It would be interesting to explore more in detail this aspect.

## VI. CONCLUSIONS

We analyzed in this paper the slow dynamics upon supercooling of TIP4P/2005 water and its connection with the thermodynamic properties determined by the presence of a LLC, already found for this model.<sup>18</sup> TIP4P/2005 is considered one of the best all atoms classic rigid potentials for water, being able to reproduce remarkably well many experimental features of this liquid, like the TMD line and the complex ices phase diagram. Also its prediction of the diffusivity as function of temperature is in good agreement with experiments.<sup>61</sup>

We found that in the mild supercooled region the TIP4P/2005 water follows the MCT predictions remarkably well. The cage effect determines a double relaxation regime with the long time decay described by a stretched exponential. Upon further supercooling hopping processes start to affect the structural relaxation, as in other glass formers. The hopping effects cause the deviation from the fragile (MCT) behavior toward a strong behavior of the liquid. Similar to what has been found for other potentials, this fragile to strong crossover takes place at the crossing of the Widom line individuated by the calculations of the maxima of the specific heat in the single phase region upon approaching the LLC.

This result is a further confirmation that in water the dynamics is intimately related to thermodynamics in all its very complex phase diagram, as made evident also from the recent results on its supercritical phase<sup>40,41</sup> where a dynamic crossover from a gas-like to a liquid-like phase has been found upon crossing the Widom Line of the liquid-gas critical point.

In the supercooled region where the thermodynamic and structural properties superpose to the glassy dynamics, when

crossing the Widom line, the low density fluctuations prevail and hopping becomes favored with respect to cage relaxation.

In this respect it is important to underline that in experiments a measure of the FSC can be considered as a proxy for the Widom line pointing to the LLC.

In comparing TIP4P<sup>46</sup> and TIP4P/2005 results in the supercooled region, we found a close similarity of the predictions in spite of the differences in the phase diagrams above the melting temperatures and in the region of the ice polymorphism. Since the pair potentials differ mainly in the distribution of the charges it seems that this plays a less relevant role in the dynamics of the system in the deep supercooled region. This would deserve a more specific analysis in the future.

Due to the clear evidence of the hopping effects in determining the activated dynamics just above the asymptotic ideal MCT transition temperature<sup>68</sup> it is worthwhile to explore more in detail the switching on of the hopping processes along the isochores explored in this paper and we plan to do it in the near future.

<sup>1</sup>V. Holten, C. E. Bertrand, M. A. Anisimov, and J. V. Sengers, *J. Chem. Phys.* **136**, 094507 (2012).

<sup>2</sup>R. S. Smith and B. D. Kay, *Nature* **398**, 788 (1999).

<sup>3</sup>H. E. Stanley, *MRS Bull.* **24**(5), 22 (1999).

<sup>4</sup>R. P. Rebelo, P. G. Debenedetti, and S. Sastry, *J. Chem. Phys.* **109**, 626 (1998).

<sup>5</sup>P. G. Debenedetti, *J. Phys.: Condens. Matter* **15**, R1669 (2003).

<sup>6</sup>P. H. Poole, F. Sciortino, U. Essmann, and H. E. Stanley, *Nature* **360**, 324 (1992).

<sup>7</sup>O. Mishima, L. D. Calvert, and E. Whalley, *Nature* **314**, 76 (1985).

<sup>8</sup>K. Winkel, M. Elsaesser, E. Mayer, and T. Loerting, *J. Chem. Phys.* **128**, 044510 (2008).

<sup>9</sup>C. U. Kim, B. Barstow, M. V. Tate, and S. M. Gruner, *Proc. Natl. Acad. Sci. U. S. A.* **106**, 4596 (2009).

<sup>10</sup>K. Winkel, E. Mayer, and T. Loerting, *J. Phys. Chem. B* **115**, 14141 (2011).

<sup>11</sup>O. Mishima and H. E. Stanley, *Nature* **392**, 164 (1998).

<sup>12</sup>O. Mishima and H. E. Stanley, *Nature* **396**, 329 (1998).

<sup>13</sup>S. Harrington, P. H. Poole, F. Sciortino, and H. E. Stanley, *J. Chem. Phys.* **107**, 7443 (1997).

<sup>14</sup>M. Yamada, S. Mossa, H. Stanley, and F. Sciortino, *Phys. Rev. Lett.* **88**, 195701 (2002).

<sup>15</sup>P. H. Poole, I. Saika-Voivod, and F. Sciortino, *J. Phys.: Condens. Matter* **17**, L431 (2005).

<sup>16</sup>D. Paschek, *Phys. Rev. Lett.* **94**, 217802 (2005).

<sup>17</sup>D. Corradini, M. Rovere, and P. Gallo, *J. Chem. Phys.* **132**, 134508 (2010).

<sup>18</sup>J. L. F. Abascal and C. Vega, *J. Chem. Phys.* **133**, 234502 (2010).

<sup>19</sup>J. Palmer, F. Martelli, Y. Liu, R. Car, A. Z. Panagiotopoulos, and P. G. Debenedetti, *Nature* **510**, 385 (2014).

<sup>20</sup>F. Smallenburg, P. Poole, and F. Sciortino, *Mol. Phys.* **113**, 2791 (2015).

<sup>21</sup>F. Smallenburg, L. Fillion, and F. Sciortino, *Nat. Phys.* **10**, 653 (2014).

<sup>22</sup>P. H. Poole, R. K. Bowles, I. Saika-Voivod, and F. Sciortino, *J. Chem. Phys.* **138**, 034505 (2013).

<sup>23</sup>J. Palmer, R. Car, and P. Debenedetti, *Faraday Discuss.* **167**, 77 (2013).

<sup>24</sup>P. Gallo and F. Sciortino, *Phys. Rev. Lett.* **109**, 177801 (2012).

<sup>25</sup>T. A. Kesselring, G. Franzese, S. V. Buldyrev, H. J. Herrmann, and H. E. Stanley, *Sci. Rep.* **2**, 474 (2012).

<sup>26</sup>Y. Liu, J. C. Palmer, A. Z. Panagiotopoulos, and P. G. Debenedetti, *J. Chem. Phys.* **137**, 214505 (2012).

<sup>27</sup>F. Sciortino, I. Saika-Voivod, and P. H. Poole, *Phys. Chem. Chem. Phys.* **13**, 19759 (2011).

<sup>28</sup>P. H. Poole, S. R. Becker, F. Sciortino, and F. W. Starr, *J. Phys. Chem. B* **115**, 14176 (2011).

<sup>29</sup>Y. Liu, A. Z. Panagiotopoulos, and P. G. Debenedetti, *J. Chem. Phys.* **131**, 104508 (2009).

<sup>30</sup>C. Buhariwalla, R. Bowles, I. Saika-Voivod, F. Sciortino, and P. Poole, *Eur. Phys. J. E* **38**, 39 (2015).

<sup>31</sup>V. Holten and M. Anisimov, *Sci. Rep.* **2**, 713 (2012).

<sup>32</sup>V. Holten, J. C. Palmer, P. H. Poole, P. G. Debenedetti, and M. A. Anisimov, *J. Chem. Phys.* **140**, 104502 (2014).



- <sup>33</sup>P. F. McMillan and E. H. Stanley, *Nat. Phys.* **6**, 479 (2010).
- <sup>34</sup>L. Xu, P. Kumar, S. V. Buldyrev, S. H. Chen, P. H. Poole, F. Sciortino, and H. E. Stanley, *Proc. Natl. Acad. Sci. U. S. A.* **102**, 16558 (2005).
- <sup>35</sup>G. Franzese and H. E. Stanley, *J. Phys.: Condens. Matter* **19**, 205126 (2007).
- <sup>36</sup>D. Fuentesvilla and M. Anisimov, *Phys. Rev. Lett.* **97**, 195702 (2006).
- <sup>37</sup>P. Kumar, G. Franzese, and H. E. Stanley, *Phys. Rev. Lett.* **100**, 105701 (2008).
- <sup>38</sup>J. Luo, L. Xu, E. Lascaris, H. E. Stanley, and S. V. Buldyrev, *Phys. Rev. Lett.* **112**, 135701 (2014).
- <sup>39</sup>V. Bianco and G. Franzese, *Sci. Rep.* **4**, 4440 (2014).
- <sup>40</sup>P. Gallo, D. Corradini, and M. Rovere, *Nat. Commun.* **5**, 5806 (2014).
- <sup>41</sup>D. Corradini, M. Rovere, and P. Gallo, *J. Chem. Phys.* **143**, 114502 (2015).
- <sup>42</sup>P. Gallo, F. Sciortino, P. Tartaglia, and S.-H. Chen, *Phys. Rev. Lett.* **76**, 2730 (1996).
- <sup>43</sup>F. Sciortino, P. Gallo, P. Tartaglia, and S.-H. Chen, *Phys. Rev. E* **54**, 6331 (1996).
- <sup>44</sup>W. Götze, *Complex Dynamics of Glass-Forming Liquids: A Mode-Coupling Theory* (Oxford University Press, Oxford, 2009).
- <sup>45</sup>R. Torre, P. Bartolini, and R. Righini, *Nature* **428**, 296 (2004).
- <sup>46</sup>P. Gallo and M. Rovere, *J. Chem. Phys.* **137**, 164503 (2012).
- <sup>47</sup>P. Gallo, D. Corradini, and M. Rovere, *J. Chem. Phys.* **139**, 204503 (2013).
- <sup>48</sup>P. Gallo, M. Rovere, and E. Spohr, *Phys. Rev. Lett.* **85**, 4317 (2000).
- <sup>49</sup>P. Gallo, M. Rovere, and E. Spohr, *J. Chem. Phys.* **113**, 11324 (2000).
- <sup>50</sup>P. Gallo, M. Rovere, and S.-H. Chen, *J. Phys. Chem. Lett.* **1**, 729 (2010).
- <sup>51</sup>P. Gallo, M. Rovere, and S.-H. Chen, *J. Phys.: Condens. Matter* **24**, 064109 (2012).
- <sup>52</sup>A. Dehaoui, B. Issenmann, and F. Caupin, *Proc. Natl. Acad. Sci. U. S. A.* **112**, 12020 (2015).
- <sup>53</sup>F. W. Starr, F. Sciortino, and H. E. Stanley, *Phys. Rev. E* **60**, 6757 (1999).
- <sup>54</sup>A. Faraone, L. Liu, C.-Y. Mou, C.-W. Yen, and S.-H. Chen, *J. Chem. Phys.* **121**, 10843 (2004).
- <sup>55</sup>L. Liu, S.-H. Chen, A. Faraone, C.-W. Yen, and C.-Y. Mou, *Phys. Rev. Lett.* **95**, 117802 (2005).
- <sup>56</sup>Y. Zhang, M. Lagi, E. Fratini, P. Baglioni, E. Mamontov, and S.-H. Chen, *Phys. Rev. E* **79**, 040201 (2009).
- <sup>57</sup>P. Gallo, M. Rovere, and S.-H. Chen, *J. Phys.: Condens. Matter* **22**, 284102 (2010).
- <sup>58</sup>D. Corradini, P. Gallo, S. V. Buldyrev, and H. Stanley, *Phys. Rev. E* **85**, 051503 (2012).
- <sup>59</sup>J. L. F. Abascal and C. Vega, *J. Chem. Phys.* **123**, 234505 (2005).
- <sup>60</sup>H. L. Pi, J. L. Aragones, C. Vega, E. G. Noya, J. L. F. Abascal, M. A. Gonzalez, and C. McBride, *Mol. Phys.* **107**, 365 (2009).
- <sup>61</sup>C. Vega, J. L. Abascal, M. Conde, and J. Aragones, *Faraday Discuss.* **141**, 251 (2009).
- <sup>62</sup>B. Hess, C. Kutzner, D. V. der Spoel, and E. Lindahl, *J. Chem. Theory Comput.* **4**, 435 (2008).
- <sup>63</sup>C. Angell, E. Finch, and P. Bach, *J. Chem. Phys.* **65**, 3063 (1976).
- <sup>64</sup>F. Prielmeier, E. Lang, R. Speedy, and H.-D. Lüdemann, *Phys. Rev. Lett.* **59**, 1128 (1987).
- <sup>65</sup>A. Scala, F. W. Starr, E. La Nave, F. Sciortino, and H. E. Stanley, *Nature* **406**, 166 (2000).
- <sup>66</sup>J. R. Errington and P. G. Debenedetti, *Nature* **409**, 318 (2001).
- <sup>67</sup>P. Gallo, R. Pellarin, and M. Rovere, *Europhys. Lett.* **57**, 212 (2002).
- <sup>68</sup>P. Gallo, A. Attili, and M. Rovere, *Phys. Rev. E* **80**, 061502 (2009).
- <sup>69</sup>J. Wong, D. A. Jahn, and N. Giovambattista, *J. Chem. Phys.* **143**, 074501 (2015).
- <sup>70</sup>P. Kumar, S. V. Buldyrev, S. R. Becker, P. H. Poole, F. W. Starr, and H. E. Stanley, *Proc. Natl. Acad. Sci. U. S. A.* **104**, 9575 (2007).
- <sup>71</sup>P. H. Poole, F. Sciortino, U. Essmann, and H. E. Stanley, *Phys. Rev. E* **48**, 3799 (1993).